ACS APPLIED POLYMER MATERIALS

pubs.acs.org/acsapm Article

Combined Reprocessability and Self-Healing in Fluorinated Acrylic-Based Covalent Adaptable Networks (CANs)

Siyang Wang, Lei Li, and Marek W. Urban*

Cite This: ACS Appl. Polym. Mater. 2022, 4, 9360−9367 Read Online

ACCESS | Metrics & More | Article Recommendations | Supporting Information

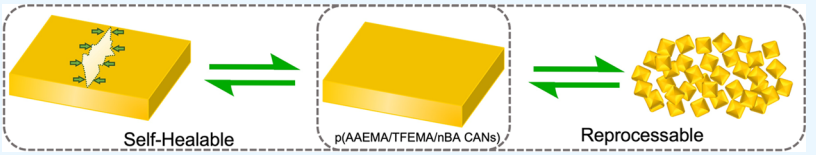

ABSTRACT: Combining reprocessing and self-healing in one material provides an opportunity for the development of sustainable materials with enhanced mechanical properties. We developed fluorinated acrylic-based covalent adaptable networks (CANs) capable of self-healing and reprocessing by copolymerizing (2-acetoacetoxy)ethyl methacrylate (AAEMA), 2,2,2-trifluoroethyl methacrylate (TFEMA), and *n*-butyl acrylate (nBA), followed by cross-linking with tris(2-aminoethyl) amine (TREN). These materials exhibit the maximum stress at break of about 16 MPa and the storage modulus of ∼2.6 GPa in the −60 to 25 °C range. Capable of complete recovery of mechanical properties, these materials are reprocessable by compression molding at 120 °C. The recovery of physical and chemical properties involves the exchange reactions between vinylogous urethane linkages and primary amines. Upon multicycle reprocessing, junction densities and stored entropic energy are also recovered and preserved. These CANs self-heal under ambient conditions. Upon damage, initially C═O groups of vinylogous urethanes respond to perturbation by conformational changes, followed by the (*E*) → (*Z*) isomerization of C═C bonds accompanied by the conformational rearrangements of the CF_3 and CH_2 moieties. This reversible process leads to the recovery of dipolar interactions that facilitates self-healing under ambient conditions. The concept of equipping materials with dynamic cross-linking and self-healing attributes can be extended to other systems.

KEYWORDS: *copolymerization, self-healable copolymers, reprocessable fluorinated acrylic thermosets, covalent adaptable networks (CANs), dipolar interactions, molecular mechanisms of self-healing*

INTRODUCTION

Attractive mechanical properties, thermal stability, resistance to chemicals, and environmental stresses in thermosetting polymeric materials make them highly desirable in many applications. On the other hand, the inherent irreversible cross-linking inhibits their processibility, which also reduces their sustainability upon bond cleavage or damage during service. To overcome these inherent disadvantages, the exploration of reprocessable and healable thermosets is highly desirable. Although noncovalent supramolecular interactions may serve this purpose, the paradigm of covalent adaptive networks (CANs)[1,2] introduced to thermoset polymers by the exchange pathways of dissociative and associative dynamic bonds created an opportunity to introduce reprocessing. Using this concept, an array of highly promising polymer systems has been introduced.[3−19]

Owing to the vast range of exceptional properties, including high solvent and heat resistance, unique electrical and mechanical properties, and low coefficients of friction,[20−22] fluoropolymers are widely used in transportation, energy storage, medicine, and other technology sectors. Many useful applications are found in microelectronics, architectural coatings, chemical-resistant pipes, valves and fittings, bearings, pump parts, and heat-shrinkable tubing as well as coatings to improve the chemical and weather resistance of metals. However, fluoropolymers are not exempted from distraction. One property that will extend their functionality is the ability to self-heal upon mechanical damage, thus extending their purposeful life span.[23] Since the high polarity of the C−F bonds considerably enhances dipolar interactions, fluorinated copolymers are promising candidates for the development of self-healing materials.[24] On the other hand, due to the inherent inertness and stability of fluoropolymers, one of the properties that is often challenging to achieve is their reprocessing. Although fluorinated polymer properties are remarkable compared to carbon-based materials, only recently the reversible covalent bonds were introduced to perfluoropolyethers.[25] If thermoplastic fluorinated copolymers are

Received: September 15, 2022
Accepted: November 17, 2022
Published: November 28, 2022

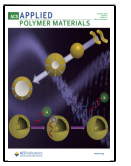

https://doi.org/10.1021/acsapm.2c01609
ACS Appl. Polym. Mater. 2022, 4, 9360−9367

Scheme 1. Synthesis of p(AAEMA/TFEMA/*n*BA) CANs: (A) p(AAEMA/TFEMA/*n*BA) Prepolymer Synthesized via RAFT Polymerization and Radical-Induced End Group Removal and (B) Cross-Linking Reaction of p(AAEMA/TFEMA/*n*BA) with TREN in 2:1 Molar Ratio (the Circle Marks a Cross-Linking Site and R═H or Repeating Unit of the p(AAEMA/TFEMA/*n*BA) Copolymer)

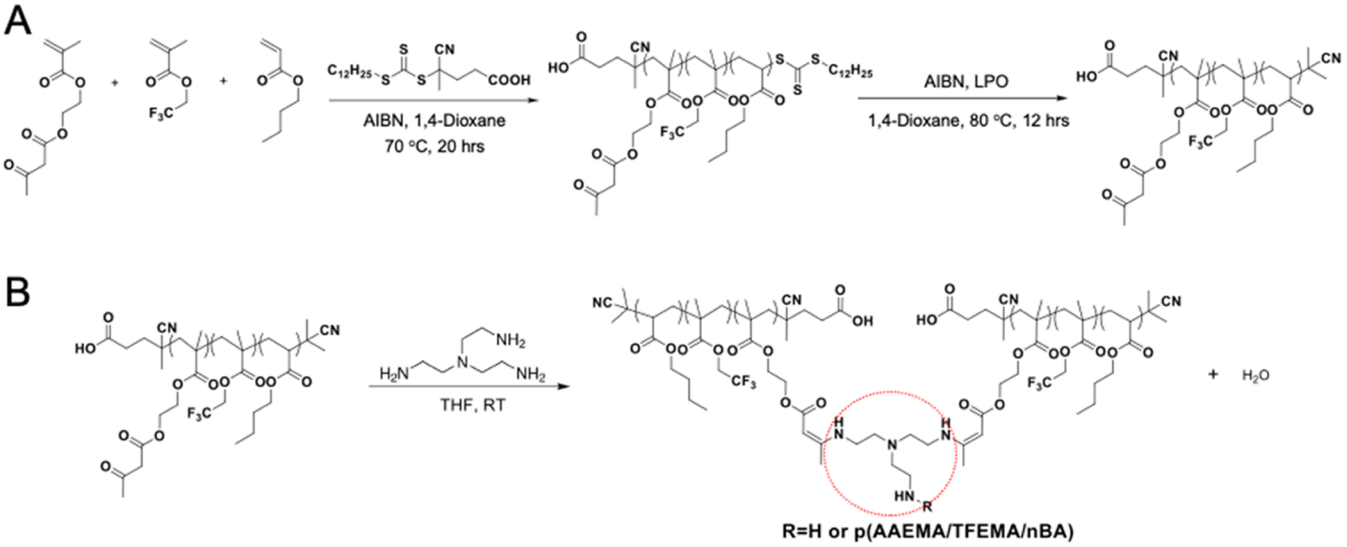

equipped with dynamic cross-links to form CANs, multiple reprocessing without sacrificing properties may be achieved.[25−28] If both self-healing and reprocessing are incorporated into one material, not only practical functions will be extended but also, when no longer needed, it can be reprocessed to serve other funtions.[29] While the combination of dipolar interactions between C—F and C═O bonds as well as CH_2/CH_3 entities in F-containing copolymers facilitates self-healing without external intervention,[24] combined reprocessablity and self-healing in these materials has not been reported. These studies outline the development of fluorinated acrylic-based copolymers that exhibit self-healing and reprocessing in one material, as well as propose molecular processes responsible for these properties.

RESULTS AND DISCUSSION

In these studies, we synthesized poly((2-acetoacetoxy)ethyl methacrylate/trifluoroethyl methacrylate/*n*-butyl acrylate) [p(AAEMA/TFEMA/*n*BA)] CANs that self-heal under ambient conditions and are reprocessable at elevated temperatures under pressure. Scheme 1 illustrates reversible addition−fragmentation chain-transfer (RAFT) copolymerization of *β*-ketoester groups containing AAEMA monomer, TFEMA monomer, and *n*BA to obtain p(AAEMA/TFEMA/*n*BA) prepolymers. During the radical-induced end group removal, thiocarbonylthio groups are replaced with cyanopropyls preventing rapid aminolysis as well as the unnecessary consumption of free primary amines when cross-linked with tris(2-aminoethyl) amines (TREN). For the AAEMA/TFEMA/*n*BA monomer molar ratio of 4.5:44:51.5, this prepolymer upon cross-linking with TREN in 2:1 molar ratio forms p(AAEMA/TFEMA/*n*BA) CANs via a condensation reaction between *β*-ketoesters and primary amines. The choice of the monomer molar ratios was determined by the following criteria: self-healability under ambient conditions (when TFEMA/*n*BA molar ratios in the vicinity of ∼45:55)[24] and reprocessability with optimized mechanical properties (AAEMA). While Figures S1, S2, and Table S1 provide a detailed characterization of synthetic and polymerization steps, Scheme 1B illustrates the process of the network formation. The appearance of the IR bands at 1600 and 1655 cm^{-1} due to C═C and N−H vibrations[30] in p(AAEMA/TFEMA/*n*BA) CANs (Figure S3, traces a and b) is attributed to the formation of vinylogous urethane linkages. While reprocessability of CANs was examined by fragmenting copolymer films into small pieces, followed by compression molding at 120 °C, self-healing was analyzed by cross-cutting intact solution-cast and reprocessed films, followed by spectroscopic analysis to elucidate molecular origins of damage−repair.

Figure 1A illustrates optical images of solution-cast p(AAEMA/TFEMA/*n*BA) CAN films that were physically destroyed into tiny pieces and compression molded at 120 °C. The reprocessing is facilitated by transamination exchange reactions, in which dynamic cross-links adjacent to free primary amines undergo the exchange at 120 °C, resulting in reformed dynamic cross-links as well as the release of free reactive amines for further exchange reactions (Figure 1B). Dynamic mechanical analysis (DMA) (Figure 1C,D) employed to examine the preservation of mechanical properties upon reprocessing shows that the storage modulus of ∼2.58 GPa in the −60 to 25 °C range (Figure 1C) and the glass transition temperature (T_g) at ∼36 °C (Figure 1D) are retained during four reprocessing cycles (R×4). Furthermore, junction densities (ν_j) and stored entropic energy (ΔS_s) values of solution-cast and reprocessed films determined from viscoelastic length transitions (VLTs) (Table S2)[31,32] remain unchanged within experimental error, signifying the preservation of mechanical properties. Tensile strain, maximum stress at break, and Young's modulus after R×4 are also maintained at ∼95, 93, and 96%, respectively (Figure 1E, traces a and c). These p(AAEMA/TFEMA/*n*BA) CANs are thermally stable up to ∼200 °C (Figure S4A), and the weight loss after 180 min at 120 °C is ∼2.3% (Figure S4B).

Optical images of p(AAEMA/TFEMA/*n*BA) CAN films shown in Figure 1F1−F4 illustrate autonomous self-healing of solution-cast and R×4 films. Mechanically damaged solution-cast (Figure 1F1) and R×4 (Figure 1F3) specimens self-heal

https://doi.org/10.1021/acsapm.2c01609
ACS Appl. Polym. Mater. 2022, 4, 9360−9367

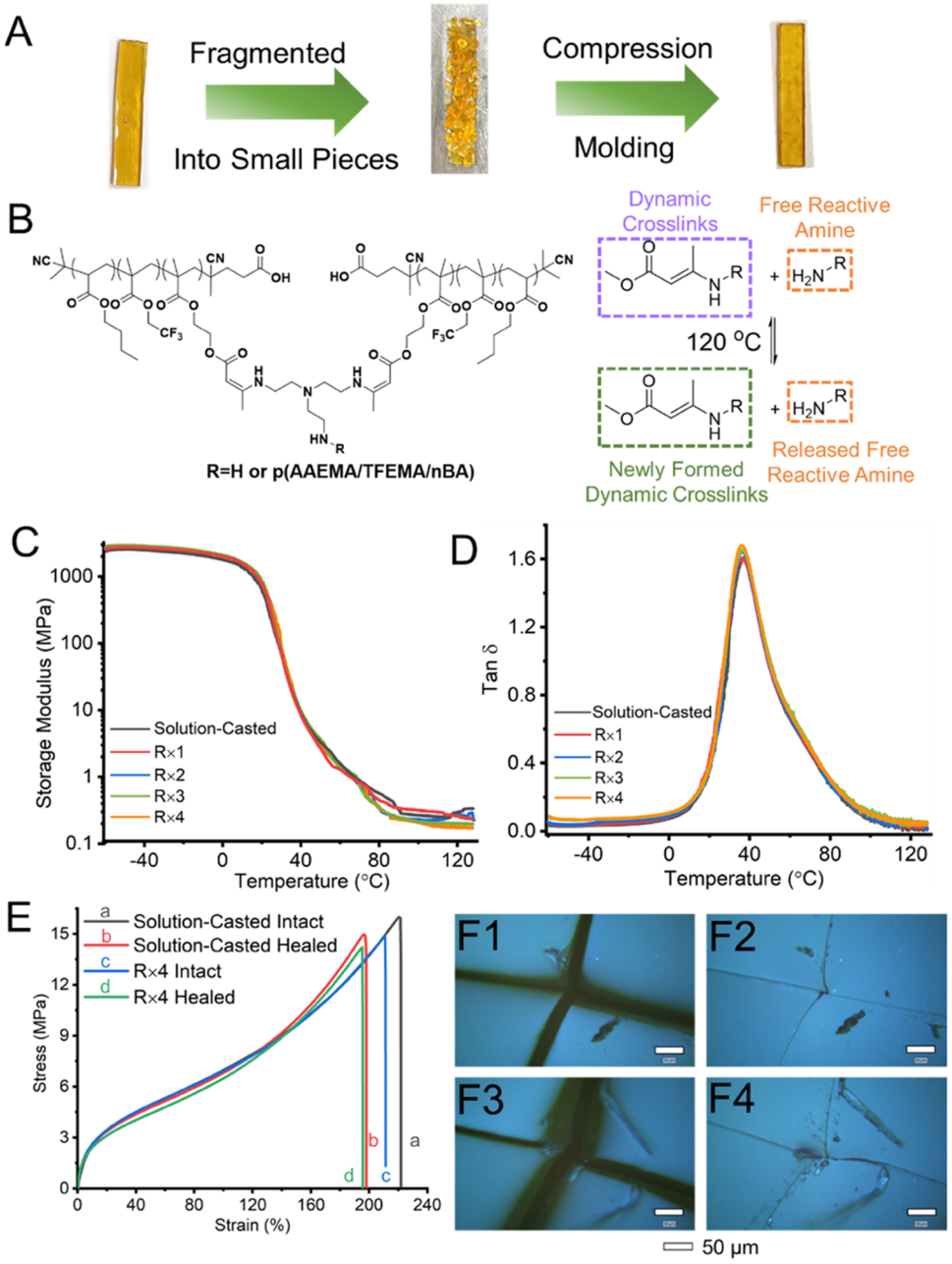

Figure 1. (A) Reprocessing of p(AAEMA/TFEMA/*n*BA) CANs via mechanical fragmentation and compression molding at 120 °C. (B) Chemical structure of p(AAEMA/TFEMA/*n*BA) CANs and the transamination exchange reaction during the reprocessing of p(AAEMA/TFEMA/*n*BA) CANs. (C) Overlayed storage modulus and (D) tan δ curves from DMA analysis. (E) Stress−strain curves of intact and self-healed specimens after 48 h: curve a, solution-cast intact; curve b, solution-cast self-healed; curve c, reprocessed × 4 times (R×4) intact; and curve d, R×4 self-healed. (F1−F4) Optical images in damage−repair process of solution-cast and reprocessed p(AAEMA/TFEMA/*n*BA) CANs: (F1) solution-cast-damaged, (F2) solution-cast-self-healed, (F3) R×4-damaged, and (F4) R×4-self-healed p(AAEMA/TFEMA/*n*BA) CANs (small scars vanish at longer times but do not impact mechanical properties).

within 48 h (~27 °C; RH ~ 53%) (Figure 1F2,F4) and stress−strain measurements (Figure 1E, traces a−d) indicate over 90% recovery of mechanical properties. The solution-cast films exhibit the tensile strain of ~221% with the maximum stress at break at ~15.98 MPa, which upon self-healing are recovered at ~90 and ~94%, respectively. The percent recoveries of damaged R×4 films are ~92 and ~95%. It should be noted that self-healing and recovery of mechanical properties are highly sensitive copolymer molar ratios. For example, in similar p(TFEMA/*n*BA) copolymers with 45:55 molar ratios,[24] 95(±4)% of stress, strain, and Young's modulus (E) recovery was observed, but tuning to the 50:50 ratio, only ~75(±5)% of recovery with the tensile strain ≈700%, maximum stress at break ≈7.3 MPa, and Young's modulus (E) of 55.6 MPa was obtained. For non-fluorinated p(MMA/*n*BA) counterparts with the molar ratios of 45:55 to 50:50,[33] the recovery of 90−100% (±5%) with the tensile strain of ~550% and the stress values of ≈8.6 MPa after self-healing was observed.

To determine molecular events that occur during the damage−repair cycle, the vibrational bands sensitive to this perturbation were identified in attenuated total reflectance

https://doi.org/10.1021/acsapm.2c01609
ACS Appl. Polym. Mater. 2022, 4, 9360−9367

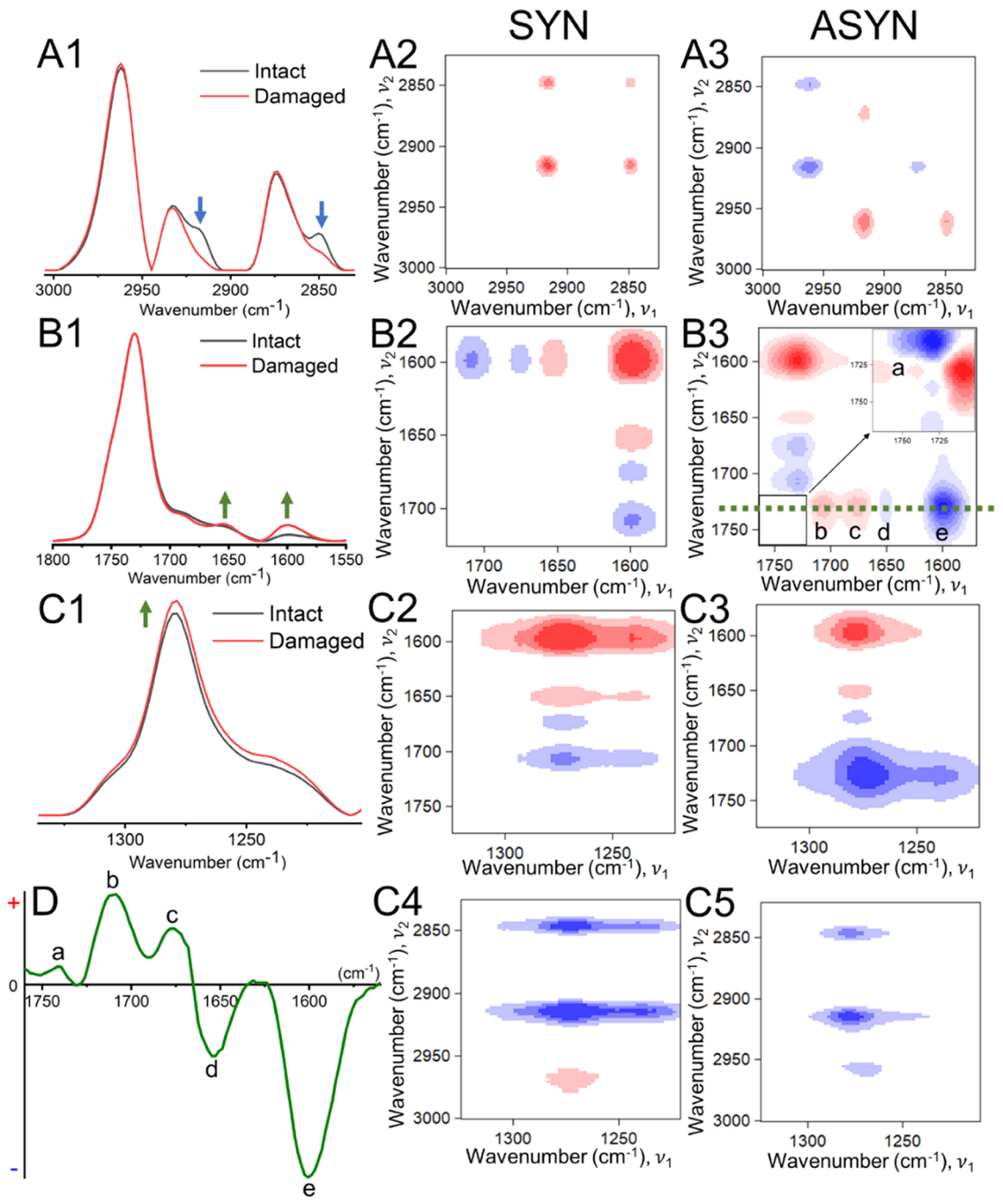

Figure 2. ATR-FTIR spectra and spectra of two-dimensional correlation spectroscopic (2D-COS) analysis for solution-cast and R×4 specimen during the damage−repair cycle. (A1) Overlayed ATR-FTIR spectra of solution-cast intact and damaged p(AAEMA/TFEMA/*n*BA) CANs in the 3000−2825 cm^{-1} range. (A2) Synchronous (SYN) and (A3) asynchronous (ASYN) spectra of solution-cast p(AAEMA/TFEMA/*n*BA) CANs in the 3000−2825 cm^{-1} range. (B1) Overlayed intact and damaged ATR-FTIR spectra of solution-cast p(AAEMA/TFEMA/*n*BA) CANs in the 1800−1550 cm^{-1} range. (B2) SYN and (B3) ASYN spectra of solution-cast p(AAEMA/TFEMA/*n*BA) CANs in the 1730−1575 cm^{-1} range. (C1) Overlayed intact and damaged ATR-FTIR spectra of solution-cast p(AAEMA/TFEMA/*n*BA) CANs in the 1325−1200 cm^{-1} range. (C2) SYN and (C3) ASYN spectra of solution-cast p(AAEMA/TFEMA/*n*BA) CANs: (ν_1) in the 1325−1200 cm^{-1} range and (ν_2) in the 1775−1575 cm^{-1} range. (C4) SYN and (C5) ASYN spectra of solution-cast p(AAEMA/TFEMA/*n*BA) CANs: (ν_1) in the 1325−1200 cm^{-1} range and (ν_2) in the 3000−2825 cm^{-1} range. (D) Correlation slicing profile at 1725 cm^{-1} of ASYN 2D-COS of solution-cast p(AAEMA/TFEMA/*n*BA) CANs.

Fourier transform infrared (ATR-FTIR) spectra. While assignments of the IR bands sensitive to the damage−repair cycle are provided in Table S3, the intensities of these vibrational bands return to nearly the same values after self-healing (Figure S5; band assignments are in Tables S4 and S5). Figure 2A1,B1,C1 illustrates ATR-FTIR spectra of the intact and damaged specimens in the C−H, C═O/C═C/N−H, and C−F stretching/bending regions, respectively. Since the concentration and composition of p(AAEMA/TFEMA/*n*BA) copolymers remain unchanged, the intensity changes are attributed to the dipole moment changes due to conformational changes of the group sensitive to the damage−repair cycles. The most pronounced intensity changes are observed in the C−H stretching regions, and although the C═C stretching

https://doi.org/10.1021/acsapm.2c01609
ACS Appl. Polym. Mater. 2022, 4, 9360−9367

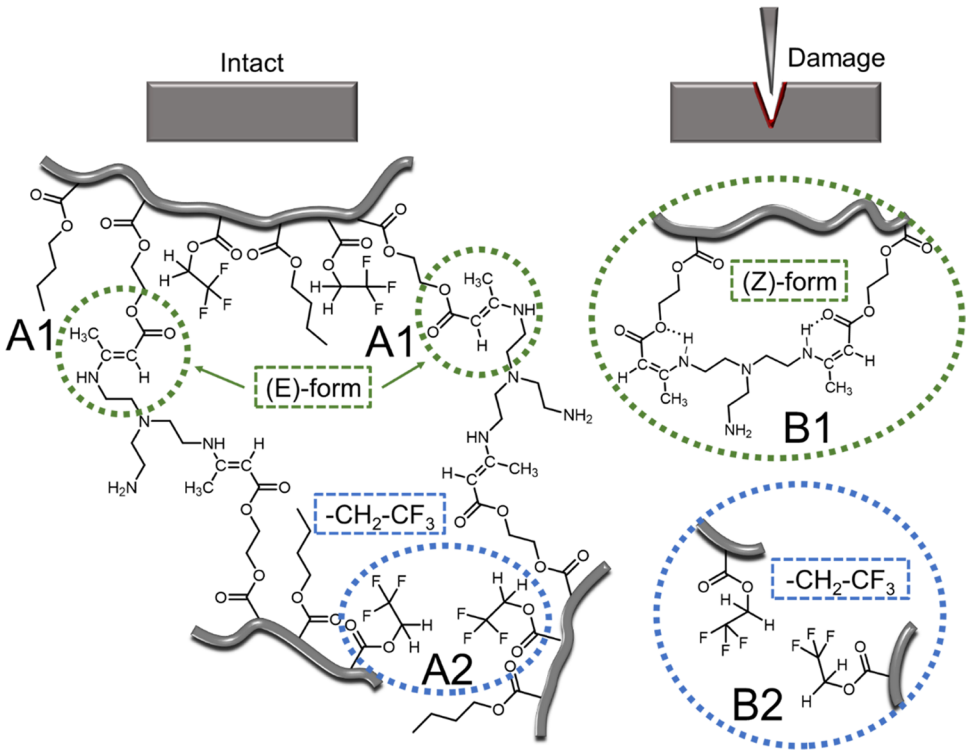

Figure 3. Schematic representations of molecular entities participating in self-healing of p(AAEMA/TFEMA/*n*BA) CANs of intact and damaged states. (A1, B1) (*E*) ⇌ (*Z*) isomerization of the C═C bond in vinylogous urethane moiety. (A2, B2) Conformational changes of $-CH_2-CF_3$ groups.

vibrations in general are relatively weak due to small dipole moment changes, as shown in Figure 2B1, the intensity of the 1600 cm^{-1} band slightly increases. Also, relatively minute intensity changes are observed in the C−F stretching vibrations upon damage (Figure 2C1). Although the increase of the C═C band intensity may suggest depolymerization, DMA analysis (Figure 1C,D) rules out this possibility because storage modulus, tan δ, v_j, and ΔS_s values remain unchanged after R×4 cycles. However, if conformational changes take place, it is hypothesized that the C═C bond may rotate.[34,35]

To test this hypothesis and determine dynamic changes resulting from the damage−repair cycle, ATR-FTIR measurement in combination with two-dimensional correlation spectroscopic (2D-COS) analysis was employed.[36,37] This approach enables the identification of molecular responses that participate in damage−repair perturbation through the analysis of synchronous (SYN) and asynchronous (ASYN) spectra. While the SYN spectra reflect simultaneous in-phase responses of chemical groups upon damage−repair, ASYN is sensitive to sequential out-of-phase events during this process. Positive cross-peaks (red) in the SYN spectra (Figure 2A2,B2,C2,C4) imply that given molecular entities responsible for IR absorbances respond in-phase in the same direction to damage−repair perturbation, and negative cross-peaks (blue) also reflect in-phase response but in opposite directions. On the other hand, ASYN analysis reflects sequential out-of-phase responses to the perturbation, in which positive (red) cross-peaks reflect responses of molecular moieties represented by *y* wavenumber in the (ν_2) spectrum that respond before other moieties represented by vibrations at *x* wavenumber in the (ν_1) spectrum. Negative cross-peaks (blue) are also attributed to sequential responses but in a reverse order.

SYN spectra shown in Figure 2A2,B2,C2,C4 illustrate positive and negative cross-peaks resulting from conformational changes of the CF_3, CH_2, C═C, and C═O groups, and Table S4 provides the summary of the cross-peaks upon damage with positive (red) and negative (blue) responses. The ASYN analysis summarized in Figure 2A3,B3,C3,C5 indicates that upon damage, CF_3, CH_2, C═C, N−H, and C═O groups respond sequentially, reflected in the positive and/or negative out-of-phase responses. These data show that, initially, three types of C═O groups (1740, 1705, and 1675 cm^{-1}) in vinylogous urethane moieties respond upon mechanical damage. Since the intensity of the C═C stretching vibrations at 1600 cm^{-1} increases (Figure 2B1), it is anticipated that this increase is associated with the symmetry changes during perturbation. Furthermore, analysis of the ASYN spectra shown in Figure 2B3 shows that the response of the C═C and N−H groups follows conformational changes of the C═O groups in vinylogous moieties. This is also reflected in the slicing profile along the 1725 cm^{-1} band shown in Figure 2D, which illustrates initial responses (positive) of C═O groups, followed by the responses of the C═C and N−H entities (negative), indicating the (*E*)- to (*Z*)-isomerization around the C═C bond. These rearrangements are followed by conformational changes of the terminal CF_3 groups of TFEMA, which trigger the symmetry changes in covalently bonded CH_2 units. These changes occur when going from intact to damaged states and are depicted in Figure 2C2−C5. The same changes are observed for damage−repair cycles of p(AAEMA/TFEMA/*n*BA) CANs after R×4 reprocessing (Figure S6).

Figure 3 summarizes molecular events during damage−repair perturbation of p(AAEMA/TFEMA/*n*BA) CANs. As shown in Figure 3A1, in an undamaged/healed state within vinylogous urethane moieties (green circle), the (*E*)-isomer

https://doi.org/10.1021/acsapm.2c01609
ACS Appl. Polym. Mater. 2022, 4, 9360−9367

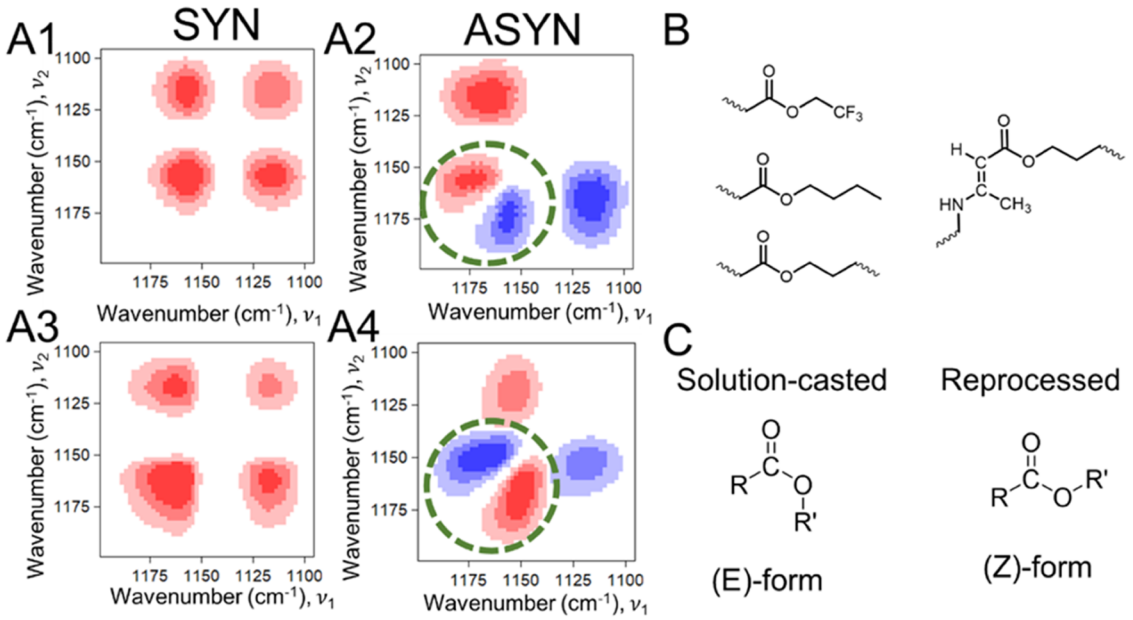

Figure 4. 2D-COS analysis for solution-cast and R×4 p(AAEMA/TFEMA/*n*BA) CANs in the range of 1050−1200 cm^{-1} upon damage. (A1) Synchronous (SYN) spectra of solution-cast p(AAEMA/TFEMA/*n*BA) CANs in the 1050−1200 cm^{-1} range. (A2) Asynchronous (ASYN) spectra of solution-cast p(AAEMA/TFEMA/*n*BA) CANs in the 1050−1200 cm^{-1} range. (A3) SYN 2D-COS spectrum of R×4 p(AAEMA/TFEMA/*n*BA) CANs in the range 1050−1200 cm^{-1}. (A4) ASYN spectra of R×4 p(AAEMA/TFEMA/*n*BA) CANs in the 1050−1200 cm^{-1} range. (B) Representative chemical structures of selected ester groups in p(AAEMA/TFEMA/*n*BA) CANs. (C) (*E*)- and (*Z*)-forms of esters in solution-cast and R×4 specimens, respectively. Note: the presence of unstable (*E*)-form esters does not impact mechanical properties in a measurable way.

geometry is favorable, and the CF_3 groups covalently attached to the CH_2 units take tetrahedral geometry (Figure 3A2, blue circle). Upon damage, vinylogous urethane moieties around the C═C bond are transformed to the (*Z*)-form (Figure 3B1; green circle) to favor inter- and intrachain H-bonding. These conformational changes are followed by CF_3 groups adapting near-planar geometries,[24] allowing H atoms on the neighboring CH_2 groups to align on both sides of the methylene carbon (Figure 3B2, blue circle). Thus, the relatively small content of AAEMA facilitates reprocessing at 120 °C and the TFEMA/*n*BA molar ratio secures self-healing under ambient conditions. Although one would expect that the cis−trans isomerization during an associative exchange of amines may affect the conformations of $COOCH_2CF_3$ moieties in the solution state, the formation of interfacial regions with significantly enhanced segmental mobilities is likely to contribute to this process. Thus, four molecular events are anticipated: (a) (*E*) ⇌ (*Z*) isomerization around the C═C bonds in vinylogous moieties, (b) exchange of inter- and intrachain H-bonding, (c) local compressions that induce structural rearrangements from tetrahedral to nearly planar geometry in the CF_3 groups, resulting in the reduction of steric hindrance between CF_3 and CH_2, and (d) increased junction densities between neighboring chains, resulting in the enhanced dipolar interactions that facilitate self-healing.

Considering vinylogous urethane moiety cross-links, it is worth pointing out that alkyl groups on amines and esters will increase the electron delocalization, thus increasing electron density on the oxygen atom of the C═O groups while reducing the C═O and C═C bond orders and promoting H-bonding. Consequently, the activation energy of the (*Z*) ⇌ (*E*) isomerization will be lower. Also, the steric hindrance between═C−CH_3 entities and *N*-alkyl groups linked to another chain in the (*Z*)-form will force the N−H groups to bend toward COOR moieties, further strengthening intrachain H-bonding that destabilizes (*Z*)-isomer relative to the strainless (*E*)-form, thus promoting self-healing.[38]

2D-COS analysis identified acrylic (TFEMA, *n*BA, AAEMA) and vinylogous urethane ester C−O stretching vibrations in p(AAEMA/TFEMA/*n*BA) CAN spectra reflected in the 1120−1165 and 1155−1175 cm^{-1} SYN and ASYN correlations, respectively (Figure 4A1−A4). Comparison of the solution-cast (Figure 4A1) and R×4 film (Figure 4A3) SYN spectra shows that upon damage−repair, the 1120 and 1165 cm^{-1} bands exhibit the same in-phase and out-of-phase responses regardless of the preparation method. On the other hand, cross-peaks at 1155 and 1175 cm^{-1} in the ASYN spectra in Figure 4A2 (solution-cast) and Figure 4A4 (R×4) (green circles) due to the C−O stretching vibrations of acrylic and vinylogous urethane esters, respectively, show reverse out-of-phase responses: from positive (red) to negative (blue). While the respective ester structures in p(AAEMA/TFEMA/*n*BA) CANs are illustrated in Figure 4B, this analysis indicates that ester groups in solution-cast films are in the (*E*)-form conformations, which are inverted to the (*Z*)-form in the R×4 films. The same 2D-COS cross-peaks are detected in R×1, R×2, and R×3 as in R×4 reprocessed specimens (Figure S7). According to the literature,[39] the preferable conformations of ester linkages are in the (*Z*)-form, particularly when R′ groups are large. However, if condensation reactions leading to cross-links in solution-cast films kinetically trap ester groups, they most likely remain in the (*E*)-form. Upon reprocessing by compression molding at elevated temperatures, ester groups will be thermodynamically equilibrated into more stable (*Z*)-form illustrated in Figure 4C.

CONCLUSIONS

To succinctly summarize these findings, we developed a class of fluorinated acrylic-based CANs that exhibit autonomous

https://doi.org/10.1021/acsapm.2c01609
ACS Appl. Polym. Mater. 2022, 4, 9360−9367

self-healing under ambient conditions and can be reprocessed at 120 °C under pressure. Using RAFT copolymerization of β-ketoester groups containing AAEMA and copolymerizing TFEMA and *n*BA monomers, p(AAEMA/TFEMA/*n*BA) polymers were obtained that upon cross-linking with TREN form CANs via a condensation reaction between β-ketoesters and primary amines. The choice of the monomers and their molar ratios was dictated by self-healability under ambient conditions, reprocessability, and mechanical properties. These materials exhibit the maximum stress at break of ∼16 MPa and the storage modulus of ∼2.6 GPa in the −60 to 25 °C range. The mechanism responsible for reprocessing is transamination exchange reactions between vinylogous urethane linkages and primary amines. These networks self-heal upon the recovery of dipolar interactions accompanied by the sequential conformational changes of C═O groups in vinylogous urethanes and (*E*) ⇌ (*Z*) isomerization of C═C bonds, followed by the conformational rearrangements of CF_3 and CH_2 moieties. It should be noted that self-healing requires no external intervention, whereas reprocessing typically does; thus, distinctly different mechanisms under different conditions are responsible for each property. Although there are literature reports assuming these two events are equivalent, in these materials, self-healability is achieved by dipolar interactions of acrylic-based repeating units, whereas reprocessability requires the presence of reversible chemical cross-links activated at elevated temperatures and pressures.

■ ASSOCIATED CONTENT

Supporting Information

The Supporting Information is available free of charge at https://pubs.acs.org/doi/10.1021/acsapm.2c01609.

Starting materials; synthetic and polymerization procedures; characterization methods (GPC, NMR, FTIR, 2D-COS, DMA, DSC, TGA); and relevant experimental details (PDF)

■ AUTHOR INFORMATION

Corresponding Author

Marek W. Urban − *Department of Materials Science and Engineering, Clemson University, Clemson, South Carolina 29634, United States;* orcid.org/0000-0002-1522-2736; Email: mareku@clemson.edu

Authors

Siyang Wang − *Department of Materials Science and Engineering, Clemson University, Clemson, South Carolina 29634, United States*

Lei Li − *Department of Materials Science and Engineering, Clemson University, Clemson, South Carolina 29634, United States*

Complete contact information is available at: https://pubs.acs.org/10.1021/acsapm.2c01609

Notes

The authors declare no competing financial interest.

■ ACKNOWLEDGMENTS

This work was supported by the National Science Foundation under the Awards DMR 2003005 and partially by OIA 1655740. The authors thank Kimberly Ivey for technical assistance in conducting thermogravimetric analysis as well as Najah Mhesn (Dr. Luzinov Group) for help with compression molding.

■ REFERENCES

(1) Kloxin, C. J.; Bowman, C. N. Covalent adaptable networks: smart, reconfigurable and responsive network systems. *Chem. Soc. Rev.* **2013**, *42*, 7161−7173.

(2) Kloxin, C. J.; Scott, T. F.; Adzima, B. J.; Bowman, C. N. Covalent adaptable networks (CANs): a unique paradigm in cross-linked polymers. *Macromolecules* **2010**, *43*, 2643−2653.

(3) McBride, M. K.; Worrell, B. T.; Brown, T.; Cox, L. M.; Sowan, N.; Wang, C.; Podgorski, M.; Martinez, A. M.; Bowman, C. N. Enabling applications of covalent adaptable networks. *Ann. Rev. Chem. Biomol. Eng.* **2019**, *10*, 175−198.

(4) Ruiz de Luzuriaga, A.; Martin, R.; Markaide, N.; Rekondo, A.; Cabañero, G.; Rodríguez, J.; Odriozola, I. Epoxy resin with exchangeable disulfide crosslinks to obtain reprocessable, repairable and recyclable fiber-reinforced thermoset composites. *Mater. Horiz.* **2016**, *3*, 241−247.

(5) Fortman, D. J.; Brutman, J. P.; De Hoe, G. X.; Snyder, R. L.; Dichtel, W. R.; Hillmyer, M. A. Approaches to sustainable and continually recyclable cross-linked polymers. *ACS Sustainable Chem. Eng.* **2018**, *6*, 11145−11159.

(6) Chen, X.; Hu, S.; Li, L.; Torkelson, J. M. Dynamic covalent polyurethane networks with excellent property and cross-link density recovery after recycling and potential for monomer recovery. *ACS Appl. Polym. Mater.* **2020**, *2*, 2093−2101.

(7) Li, L.; Chen, X.; Torkelson, J. M. Reprocessable polymer networks via thiourethane dynamic chemistry: recovery of cross-link density after recycling and proof-of-principle solvolysis leading to monomer recovery. *Macromolecules* **2019**, *52*, 8207−8216.

(8) Chen, X.; Li, L.; Torkelson, J. M. Recyclable polymer networks containing hydroxyurethane dynamic cross-links: Tuning morphology, cross-link density, and associated properties with chain extenders. *Polymer* **2019**, *178*, No. 121604.

(9) Cheng, K.; Chortos, A.; Lewis, J. A.; Clarke, D. R. Photoswitchable Covalent Adaptive Networks Based on Thiol−Ene Elastomers. *ACS Appl. Mater. Interfaces* **2022**, *14*, 4552−4561.

(10) Lyu, Z.; Sun, S.; Wu, T. Highly stretchable covalent adaptive networks enabled by dynamic boronic diester linkages with nitrogen→ boron coordination. *J. Polym. Sci.* **2022**, *60*, 72−80.

(11) Li, L.; Chen, X.; Torkelson, J. M. Covalent adaptive networks for enhanced adhesion: Exploiting disulfide dynamic chemistry and annealing during application. *ACS Appl. Polym. Mater.* **2020**, *2*, 4658−4665.

(12) Ricarte, R. G.; Tournilhac, F.; Leibler, L. Phase separation and self-assembly in vitrimers: Hierarchical morphology of molten and semicrystalline polyethylene/dioxaborolane maleimide systems. *Macromolecules* **2019**, *52*, 432−443.

(13) An, Q.; Wessely, I. D.; Matt, Y.; Hassan, Z.; Bräse, S.; Tsotsalas, M. Recycling and self-healing of dynamic covalent polymer networks with a precisely tuneable crosslinking degree. *Polym. Chem.* **2019**, *10*, 672−678.

(14) Jin, K.; Banerji, A.; Kitto, D.; Bates, F. S.; Ellison, C. J. Mechanically robust and recyclable cross-linked fibers from melt blown anthracene-functionalized commodity polymers. *ACS Appl. Mater. Interfaces* **2019**, *11*, 12863−12870.

(15) Ishibashi, J. S. A.; Kalow, J. A. Vitrimeric silicone elastomers enabled by dynamic meldrum's acid-derived cross-links. *ACS Macro Lett.* **2018**, *7*, 482−486.

(16) Spiesschaert, Y.; Guerre, M.; De Baere, I.; Van Paepegem, W.; Winne, J. M.; Du Prez, F. E. Dynamic curing agents for amine-hardened epoxy vitrimers with short (re)processing times. *Macromolecules* **2020**, *53*, 2485−2495.

(17) Scheutz, G. M.; Lessard, J. J.; Sims, M. B.; Sumerlin, B. S. Adaptable crosslinks in polymeric materials: resolving the intersection of thermoplastics and thermosets. *J. Am. Chem. Soc.* **2019**, *141*, 16181−16196.

(18) Denissen, W.; De Baere, I.; Van Paepegem, W.; Leibler, L.; Winne, J.; Du Prez, F. E. Vinylogous urea vitrimers and their application in fiber reinforced composites. *Macromolecules* **2018**, *51*, 2054−2064.
(19) Mao, J.; Hai, Y.; Ye, H.; You, L. Adaptive Covalent Networks Enabled by Dual Reactivity: The Evolution of Reversible Covalent Bonds, Their Molecular Assemblies, and Guest Recognition. *J. Org. Chem.* **2020**, *85*, 5351−5361.
(20) Améduri, B.; Boutevin, B.; Kostov, G. Fluoroelastomers: synthesis, properties and applications. *Prog. Polym. Sci.* **2001**, *26*, 105−187.
(21) Vitale, A.; Bongiovanni, R.; Ameduri, B. Fluorinated oligomers and polymers in photopolymerization. *Chem. Rev.* **2015**, *115*, 8835−8866.
(22) Cui, Z.; Drioli, E.; Lee, Y. M. Recent progress in fluoropolymers for membranes. *Prog. Polym. Sci.* **2014**, *39*, 164−198.
(23) Wang, S.; Urban, M. W. Self-healing polymers. *Nat. Rev. Mater.* **2020**, *5*, 562−583.
(24) Wang, S.; Urban, M. W. Self-Healable Fluorinated Copolymers Governed by Dipolar Interactions. *Adv. Sci.* **2021**, *8*, No. 2101399.
(25) Guerre, M.; Taplan, C.; Nicolaÿ, R.; Winne, J. M.; Du Prez, F. E. Fluorinated vitrimer elastomers with a dual temperature response. *J. Am. Chem. Soc.* **2018**, *140*, 13272−13284.
(26) Montarnal, D.; Capelot, M.; Tournilhac, F.; Leibler, L. Silica-like malleable materials from permanent organic networks. *Science* **2011**, *334*, 965−968.
(27) Lessard, J. J.; Garcia, L. F.; Easterling, C. P.; Sims, M. B.; Bentz, K. C.; Arencibia, S.; Savin, D. A.; Sumerlin, B. S. Catalyst-free vitrimers from vinyl polymers. *Macromolecules* **2019**, *52*, 2105−2111.
(28) Podgórski, M.; Fairbanks, B. D.; Kirkpatrick, B. E.; McBride, M.; Martinez, A.; Dobson, A.; Bongiardina, N. J.; Bowman, C. N. Toward stimuli-responsive dynamic thermosets through continuous development and improvements in covalent adaptable networks (CANs). *Adv. Mater.* **2020**, *32*, No. 1906876.
(29) Wang, S.; Li, L.; Liu, Q.; Urban, M. W. Self-Healable Acrylic-Based Covalently Adaptable Networks. *Macromolecules* **2022**, *55*, 4703−4709.
(30) Urban, M. W. *Vibrational Spectroscopy of Molecules and Macromolecules on Surfaces*; Wiley-Interscience, 1993.
(31) Hornat, C. C.; Yang, Y.; Urban, M. W. Quantitative predictions of shape-memory effects in polymers. *Adv. Mater.* **2017**, *29*, No. 1603334.
(32) Hornat, C. C.; Urban, M. W. Entropy and interfacial energy driven self-healable polymers. *Nat. Commun.* **2020**, *11*, No. 1028.
(33) Urban, M. W.; Davydovich, D.; Yang, Y.; Demir, T.; Zhang, Y.; Casabianca, L. Key-and-lock commodity self-healing copolymers. *Science* **2018**, *362*, 220−225.
(34) Barrows, S. E.; Eberlein, T. H. Understanding rotation about a C═C double bond. *J. Chem. Educ.* **2005**, *82*, No. 1329.
(35) Bühringer, M. U.; Padberg, K.; Phleps, M. D.; Maid, H.; Placht, C.; Neiss, C.; Ferguson, M. J.; Goerling, A.; Tykwinski, R. R. Double bonds? Studies on the barrier to rotation about the cumulenic C═C bonds of tetraaryl [n] cumulenes (n = 3, 5, 7, 9). *Angew. Chem., Int. Ed.* **2018**, *57*, 8321−8325.
(36) Lasch, P.; Noda, I. Two-dimensional correlation spectroscopy (2D-COS) for analysis of spatially resolved vibrational spectra. *Appl. Spectrosc.* **2019**, *73*, 359−379.
(37) Park, Y.; Noda, I.; Jung, Y. M.Application of Two-Dimensional Correlation Spectroscopy (2D-COS) in Polymer Studies. In *Spectroscopic Techniques for Polymer Characterization: Methods, Instrumentation, Applications*; Wiley-VCH GmbH, 2021; Chapter 9, pp 259−296.
(38) Gómez Sánchez, A.; Valle, A.; Bellanato, J. Infrared and nuclear magnetic resonance absorption and isomerism of 3-aminocrotonic esters. Part II. *J. Chem. Soc., Perkin Trans. 2* **1973**, *1*, 15−20.
(39) Pawar, D. M.; Khalil, A. A.; Hooks, D. R.; Collins, K.; Elliott, T.; Stafford, J.; Smith, L.; Noe, E. A. E and Z conformations of esters, thiol esters, and amides. *J. Am. Chem. Soc.* **1998**, *120*, 2108−2112.

https://doi.org/10.1021/acsapm.2c01609
ACS Appl. Polym. Mater. 2022, 4, 9360−9367